Significant Change of Extratropical Natural Variability Associated with Tropical ENSO Anomaly

WILBUR Y. CHEN

Climate Prediction Center, NOAA/NWS/NCEP, Washington, D.C.

(Manuscript received 26 February 2003, in final form 8 December 2003)

ABSTRACT

The natural variability over the North Pacific, where the influence of tropical El Niño–Southern Oscillation (ENSO) events is substantial, is examined to determine whether there is a large change owing to a difference in the ENSO forcing anomaly. The hindcast ensemble runs of the Seasonal Forecast Model of the National Centers for Environmental Prediction are analyzed for this assessment. Four sets of 10-member ensemble hindcasts out to 7 months with T42 horizontal resolution and another four sets with T62 resolution are examined in detail. The results consistently indicate that the natural variability, on both seasonal and monthly time scales, is significantly smaller during El Niño boreal winters than during La Niña boreal winters. The implication is that the predictability on both seasonal and monthly time scales over the North Pacific is potentially higher during El Niño winters than during La Niña winters.

1. Introduction

It is well documented that the extratropical atmosphere responds prominently to heating anomalies in the Tropics (e.g., Horel and Wallace 1981; Hoskins and Karoly 1981; Rasmusson and Wallace 1983; Wallace and Blackmon 1983). When the anomalous tropical forcing is El Niño (La Niña)–like, the North Pacific jet stream strengthens (weakens) and extends eastward and slightly southward (retracts backward). Accompanying this change are below (above) normal northeastern Pacific geopotential heights (e.g., Wallace and Blackmon 1983). There is no controversy with respect to the existence of an ENSO influence in the northeast Pacific. What is not universally agreed upon is the effect of ENSO upon the natural variability over the ENSO-sensitive region of the northeast Pacific. For example, Chen and van den Dool (1995, 1997a,b, 1999) showed that, because of the widely different basic states and the resulting barotropic energy conversion between the low-frequency disturbances and the basic state, the natural variability should be noticeably different—much larger during La Niña boreal winters than El Niño winters. By means of a series of numerical experiments, Lin and Derome (1996) confirmed that the forecast skill is higher (lower) for anomalously negative (positive) height environments over the northeast Pacific. Based on ensemble simulations made with an atmospheric general circulation model, Schubert et al. (2001) also concluded that the seasonal noise kinetic energy over the North Pacific was more than 2 times larger for the 1989 La Niña winter than for the 1983 El Niño winter. On the other hand, Sardeshmukh et al. (2000) and Compo et al. (2001) demonstrated larger natural variability on both monthly and seasonal time scales for an El Niño type of tropical forcing than for a La Niña type. Furthermore, Kumar et al. (2000) report that ''although the natural variability tends to be suppressed during warm events, a systematic increase during cold events is not found.''

The issue of significant changes in the natural variability of the atmosphere is an important one. For long-range forecasting, the predictability depends upon not only the strength of the climate signal but also on the magnitude of the omnipresent climate noise (the natural variability). Beside being of an academic interest, changes of natural variability are also of practical importance. In this short article, we evaluate the most recent results from the newly developed Seasonal Forecast Model (SFM) used at the National Centers for Environmental Prediction (NCEP), as part of an extensive investigation into the model's capability for long-range predictions (seasonal and beyond).

2. Model and data used

The Seasonal Forecast Model was developed by the seasonal prediction modeling group at NCEP (headed by M. Kanamitsu). For a detailed description of the model refer to Kanamitsu et al. (2002). Very briefly, with the scheme used placed inside the parentheses, the

Corresponding author address: Dr. Wilbur Y. Chen, Climate Prediction Center, National Centers for Environmental Prediction, 5200 Auth Road, Camp Springs, MD 20746.
E-mail: wilbur.chen@noaa.gov

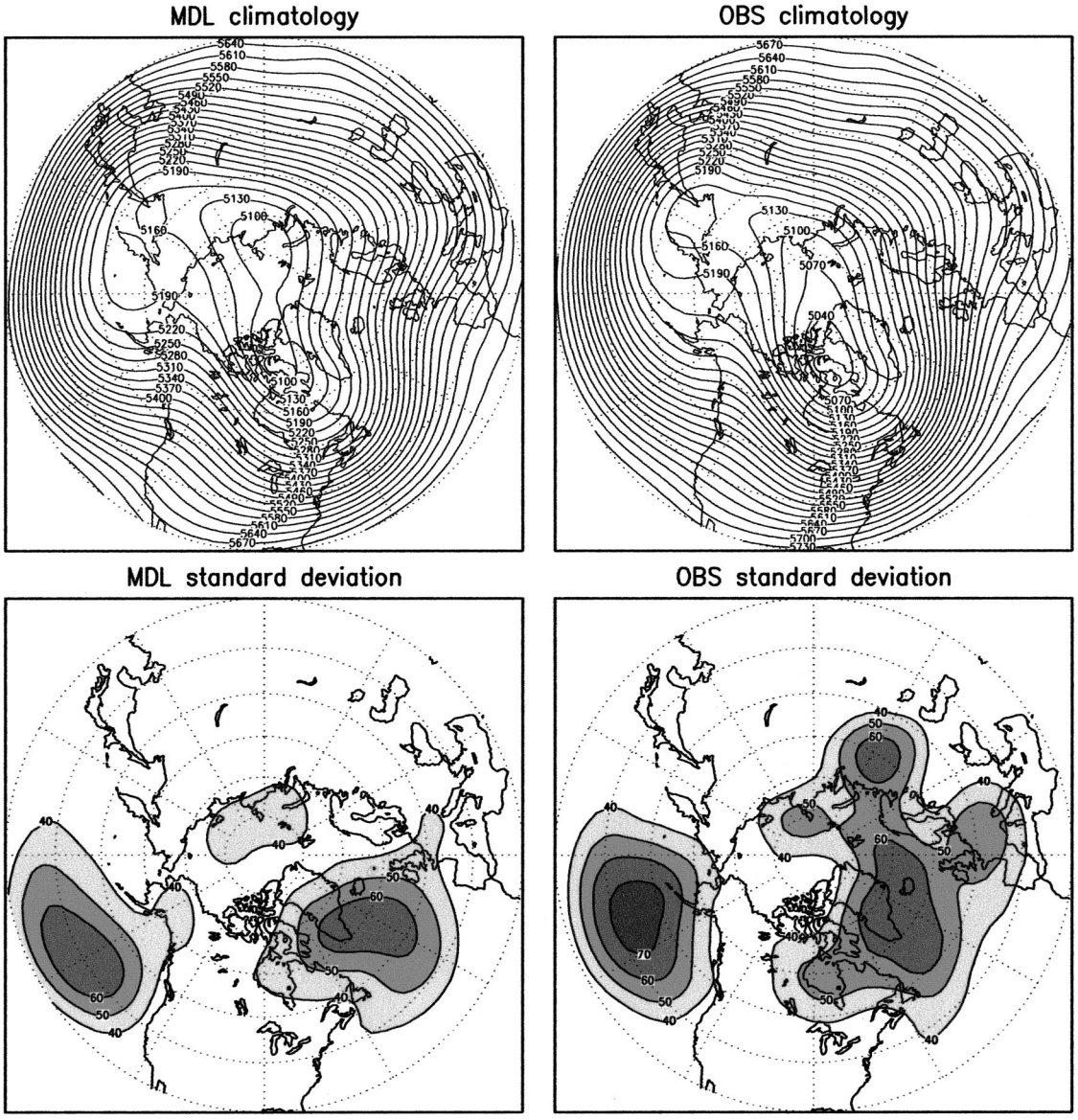

FIG. 1. Simulations of the 500-hPa geopotential height (Z500) climatology and variability for the boreal winters (JFM). Hindcasts for JFM were initialized in each preceding December from 1979 to 1999 and run out to 7 months. Standard deviations smaller than 40 m were suppressed for clarity.

particulars of the model are resolution (T42L28), convection (relaxed Arakawa–Schubert scheme, Moorthi and Suarez 1992), short- and longwave radiation (Chow 1992), clouds (Slingo 1987), planetary boundary layer (nonlocal), gravity wave drag (Alpert et al. 1988), land processes (Oregon State University two-layer soil), orography (smoothed mean), ozone (climatology), and sea surface temperatures (ensemble mean of 16-member coupled forecast).

As mentioned above, NCEP is undertaking an extensive evaluation of the model's capability on long-range prediction. As part of this goal, three major categories of model simulations have been conducted:

1) An ensemble of 10 Atmospheric Model Intercomparison Project (AMIP) 50-yr runs, in which the observed sea surface temperatures (SSTs) for the last 50 years were used as the major lower-boundary

→

FIG. 2. Simulations of the Z500 JFM mean response to El Niño, La Niña, and neutral types of tropical forcing: anomalous positive height responses (solid curves) and anomalous negative responses (dashed curves). Anomalies less than 20 m are suppressed for clarity.

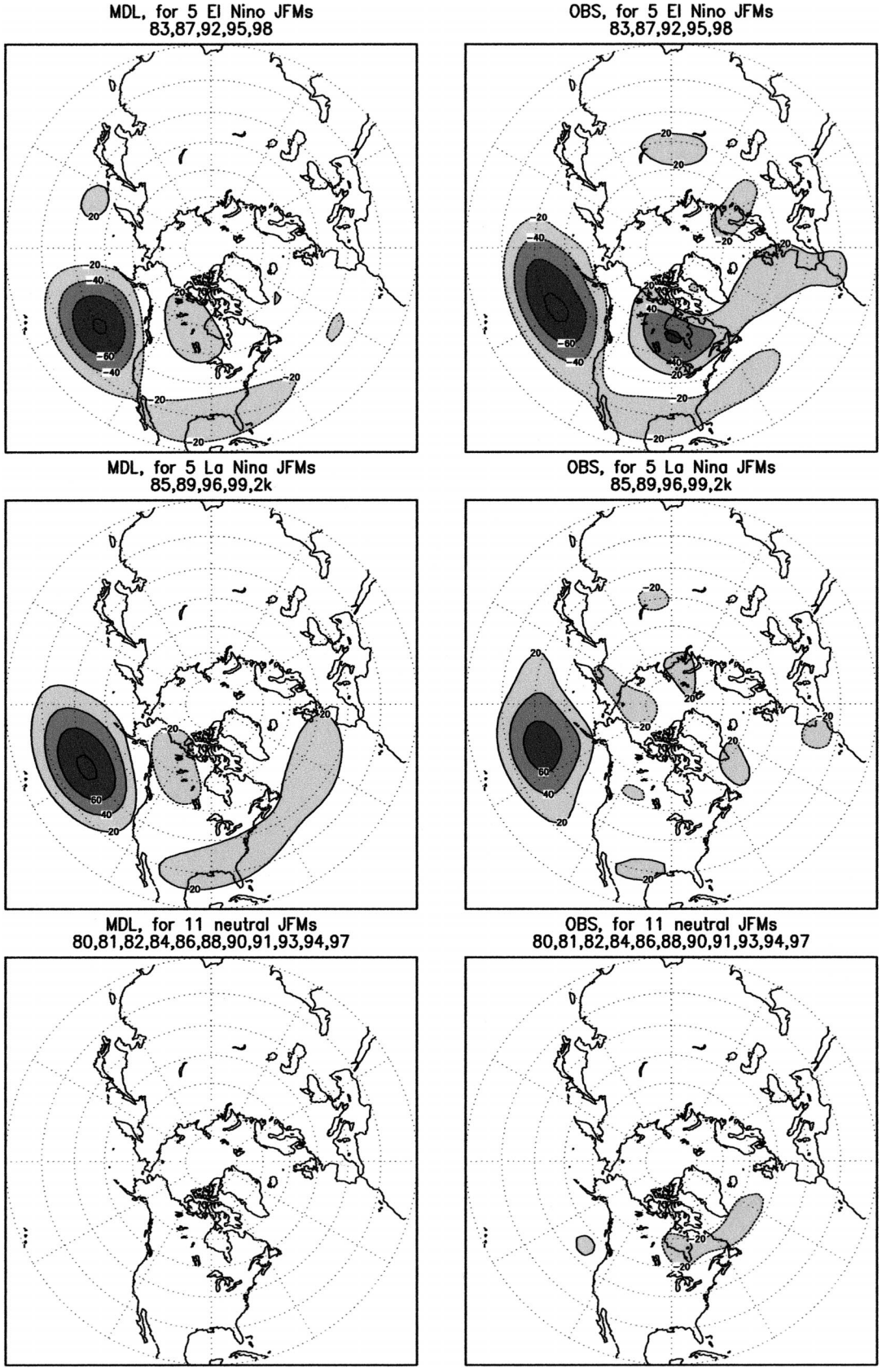
MDL, for 5 El Nino JFMs
83,87,92,95,98
OBS, for 5 El Nino JFMs
83,87,92,95,98
MDL, for 5 La Nina JFMs
85,89,96,99,2k
OBS, for 5 La Nina JFMs
85,89,96,99,2k
MDL, for 11 neutral JFMs
80,81,82,84,86,88,90,91,93,94,97
OBS, for 11 neutral JFMs
80,81,82,84,86,88,90,91,93,94,97

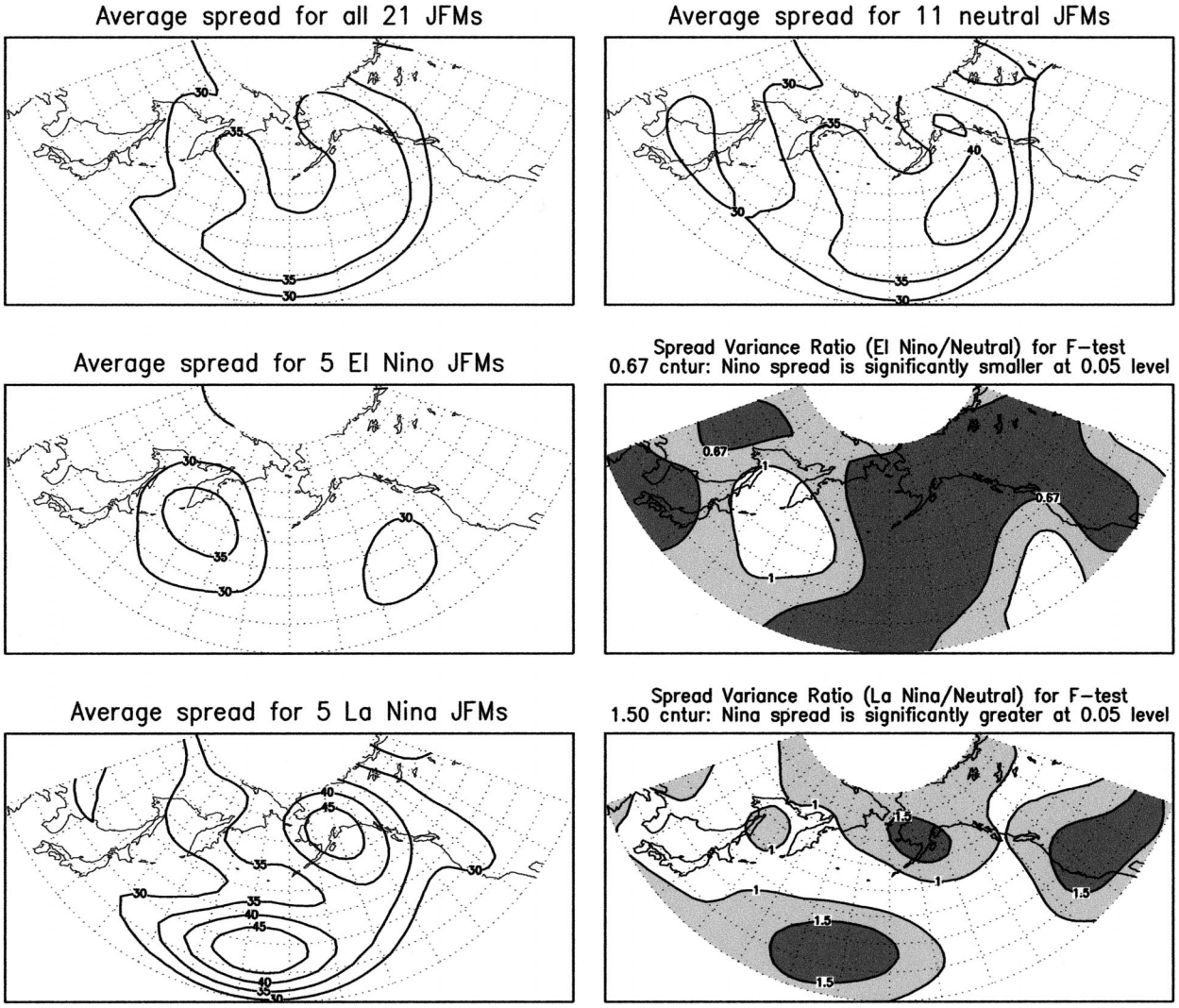

FIG. 3. Comparison of the magnitude of natural variability. Spread is defined as the standard deviation of the ensemble members from their mean. Shaded areas denote regions for which the spread variance ratio is smaller (greater) than 1.0 for El Niño (La Niña) composites. Darker shades represent regions where the ratio is statistically significant at 0.05 level by an *F* test.

forcing. Several other 50-yr runs were also conducted for other model behavior examinations.

2) An ensemble of 10 7-month hindcasts for every month of the last 21 years (1979–99). These hindcasts are also forced by the prescribed SSTs.
3) An ensemble of 20 7-month forecasts for every new month as time goes on. For these, the forecasted SSTs are used.

Despite the existence of some systematic biases, the hindcasts on seasonal time scales do show skill. When validated against the NCEP–NCAR reanalyses (Kalnay et al. 1996), the simulations are reasonable, especially for the last two decades when the reanalysis data are more trustworthy (Kanamitsu et al. 2002).

For this brief report, we focus on the significant changes in the extratropical natural variability as the tropical forcing undergoes a change from an El Niño–to a La Niña–type forcing, or vice versa. The model data used were taken from the hindcast ensemble runs mentioned above. For validation of the target winter seasons, the NCEP–NCAR reanalyses from 1980 to 2000 (Kalnay et al. 1996) were used.

3. Climatology and standard deviation: Model versus observed

The simulations of the 500-hPa geopotential height ($Z500$) climatology and variability are examined first. Figure 1 compares the results between the model (MDL) and the observed (OBS). The target season of the simulation is January–March (JFM). The period covered is from 1979/80 to 1999/2000. The MDL results were obtained from the 10-member ensemble hindcasts initialized in various months (Sep–Dec) prior to the ensuing JFM.

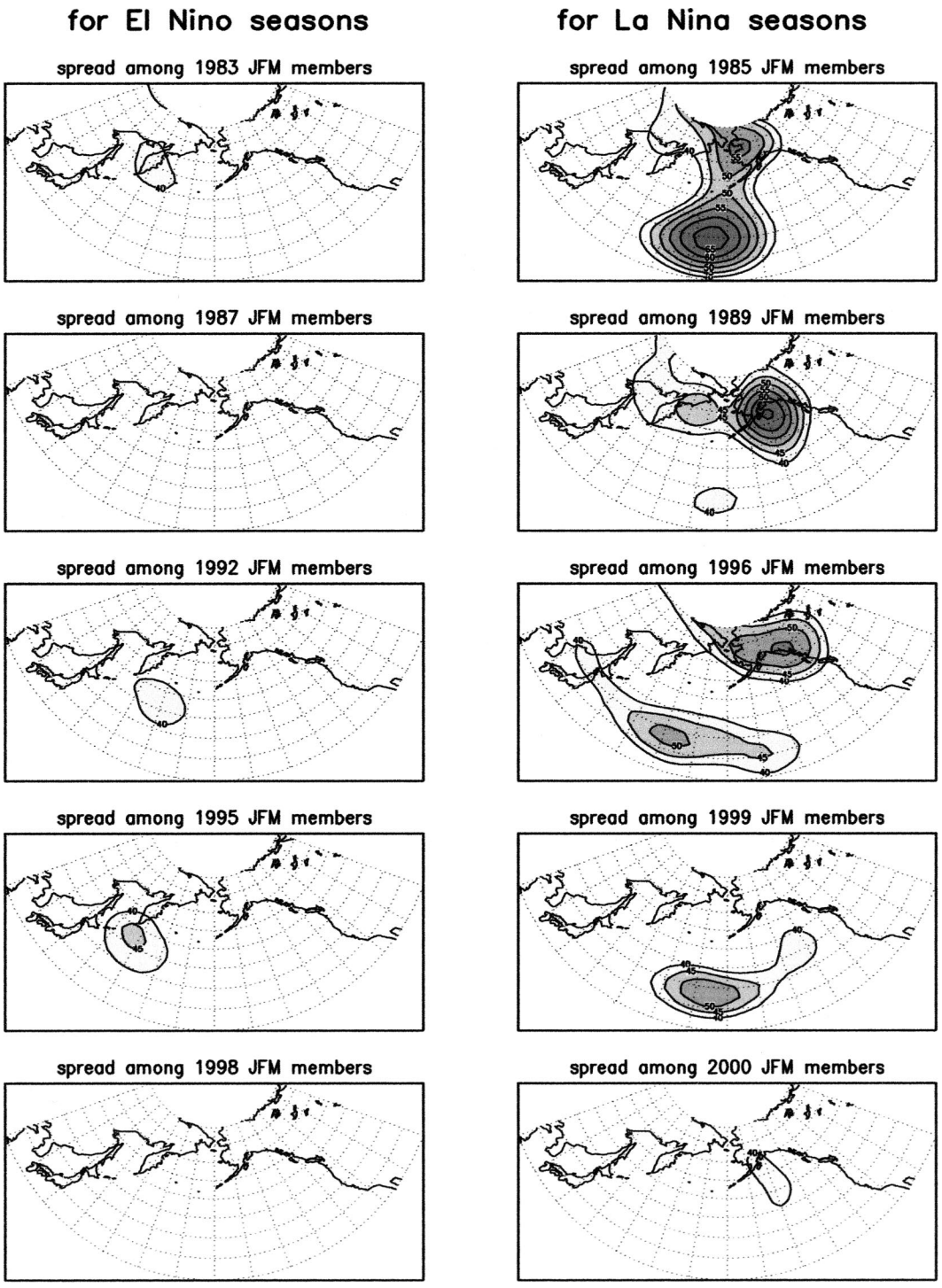

FIG. 4. Comparison of natural variability for individual ENSO events. Contour interval is 5 m, and spreads less than 40 m are suppressed for clarity.

The gross features are similar between the MDL and the OBS. The model climatology shows a stronger ridge on the western side of the continents while the polar low is not as deep. Most relevant to this article is the good simulation of the model's variability, as shown in the lower panels. The standard deviation (SD) of each individual run was obtained first. The average of 10 runs was then obtained and compared in this figure. As shown, the model's SD is weaker in general. The smaller variability is most apparent over the northeastern Pa-

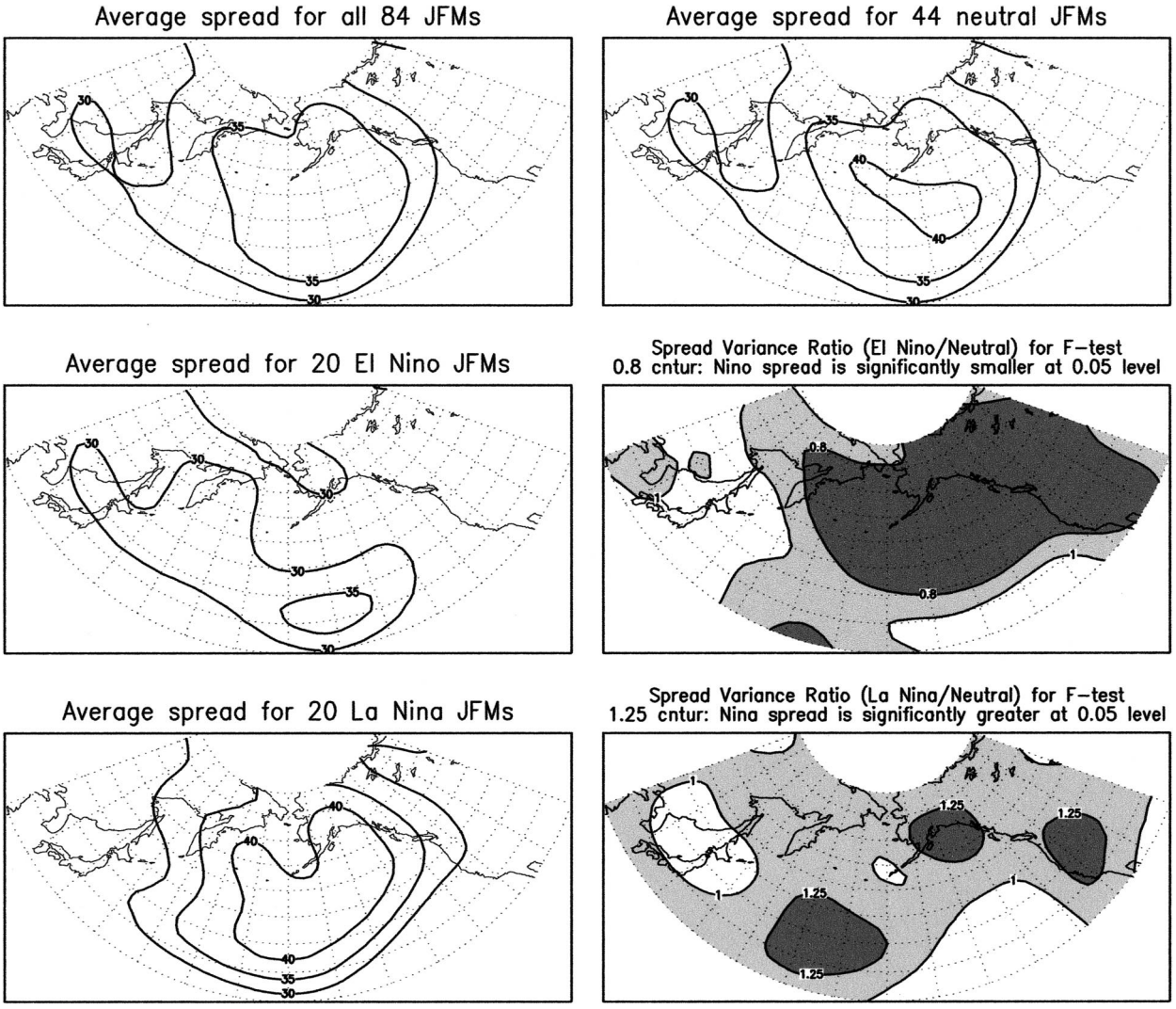

FIG. 5. Similar to Fig. 3 except for the average of four sets of runs. Each produces the JFM hindcasts, but initialized from a different month: Sep, Oct, Nov, and Dec, respectively. Note that the darker shades represent where the El Niño (La Niña) composite is significantly smaller (larger) than neutral one at the 0.05 significance level *F* test.

cific, Europe, and eastern Siberia. Smaller variability is one of the weaknesses of the present model. However, the gross resemblance of the variability pattern with observations provides us an opportunity to examine further the modification of its natural variability while its mean flow undergoes a change from an El Niño to a La Niña type.

4. Simulation of the extratropical mean response to tropical anomalous forcing

Before examining the changes in natural variability, we would like to get a feel as to how close the model mean response is to the anomalous tropical forcing, as well as which region of the globe is most sensitive to an ENSO anomalous forcing, so that the relationship between the mean response and the associated natural variability can be determined over this ENSO-sensitive region. For this purpose, three categories of JFM atmospheric circulations are examined. They are the El Niño, La Niña, and neutral type of atmospheric basic state.

The years in which an ENSO episode occurred have been sorted out and posted on the Climate Prediction Center's Web site. Over the period from 1980 to 2000, five moderate to strong El Niño episodes in the JFM season can be identified. They are in 1983, 1987, 1992, 1995, and 1998. In order to facilitate a better comparison, an equal number of the five strongest La Niña events were also selected. They occurred in 1985, 1989, 1996, 1999, and 2000. The remaining 11 JFM seasons over this period are treated as ENSO neutral years. They are 1980, 1981, 1982, 1984, 1986, 1988, 1990, 1991, 1993, 1994, and 1997.

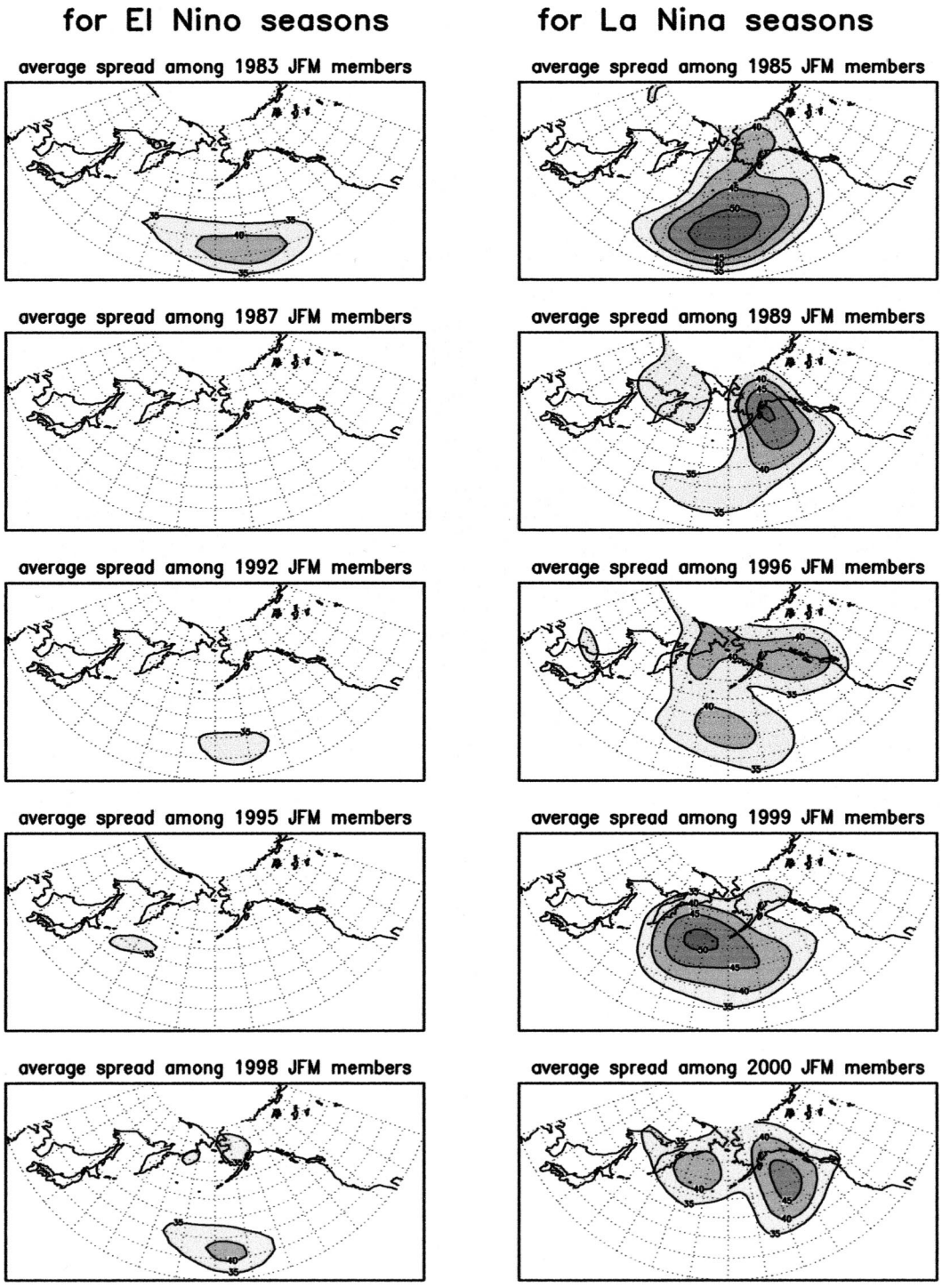

FIG. 6. Similar to Fig. 4 except for the average of four sets of hindcast runs, mentioned in Fig. 5.

Figure 2 contrasts the model mean response with those of the observed for each ENSO category. The model mean response appears to be well behaved. The height anomalies over the northeast Pacific are most dominant for both the OBS and the MDL. The MDL's mean response over this sensitive region is well simulated. A bias of the MDL tends to yield a more linear response than the real atmosphere over this region, and over North America and the North Atlantic. However, the ENSO signals over these two latter regions are much weaker than the sensitive northeast Pacific sector. For neutral winters, there is little ENSO signal to speak of,

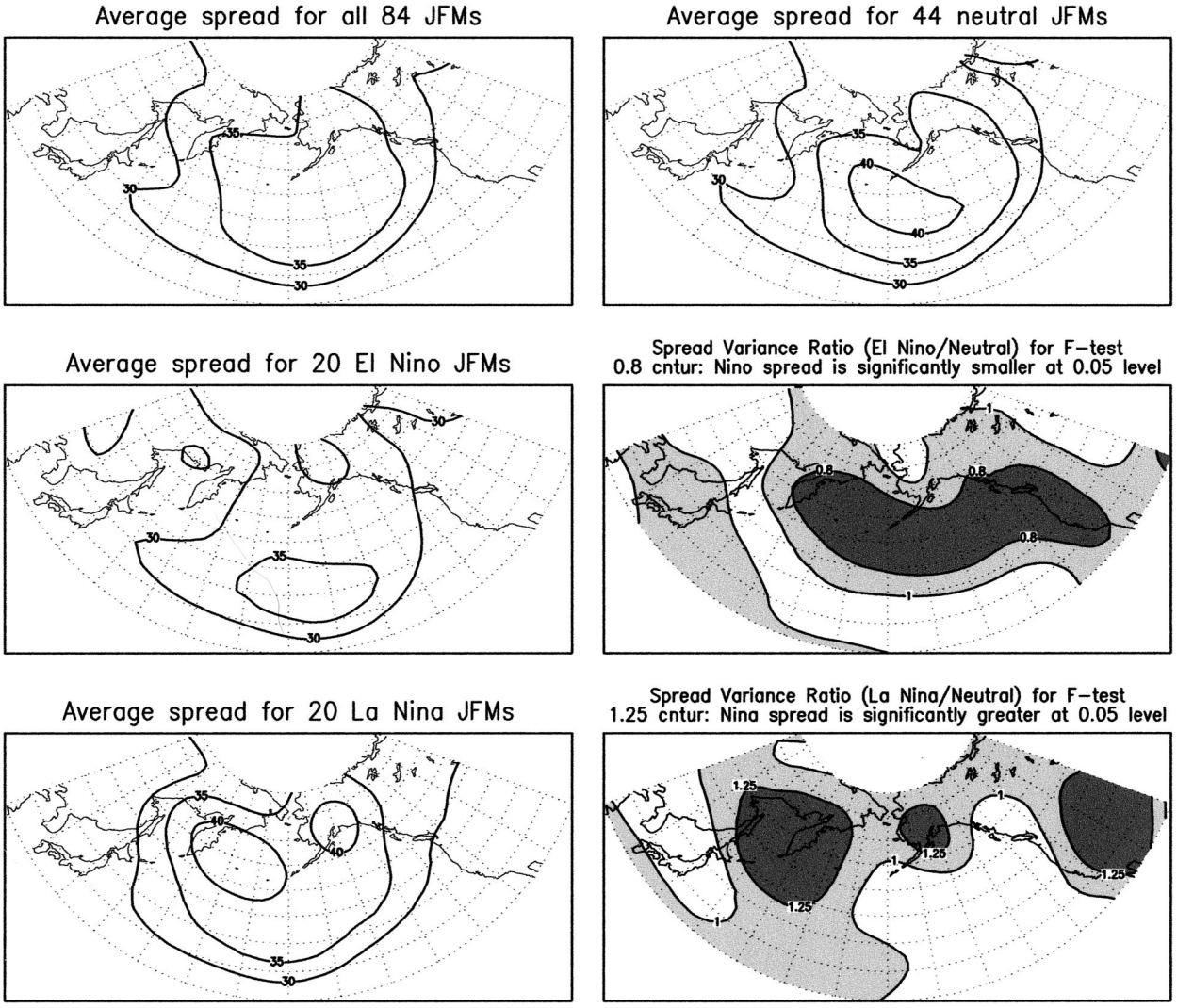

FIG. 7. Similar to Fig. 5 except for the upgraded ensemble runs with T62 resolution.

as would be expected from the near-zero ENSO anomalous forcing. The simulations faithfully reflect this feature.

Since the mean responses are well simulated, we proceed to investigate the change of the natural variability associated with a change in ENSO anomalous forcing. Here we resort to the model run's unique advantage to generate as many realizations as computer resources allow, for which the OBS data are unable to provide owing to its single realization.

5. Modification of the extratropical natural variability

As the mean response changes from an El Niño to a La Niña type of basic state, we investigate whether the magnitude of the associated natural variability also changes. Figure 3 shows the results. The spread in terms of the standard deviation among the 10 runs for each JFM is obtained first. The composites for all 21 winters, 5 El Niños, 5 La Niñas, and 11 neutral JFMs were then constructed. As shown in the figure, while the El Niño composite yields mostly less than 30 m in its spread over the North Pacific, where the ENSO signals are most sensitive and substantial, the La Niña composite shows a much larger magnitude and spatial extent. The neutral year composite is very similar to the averaged spread of all 21 JFMs in both magnitude and pattern.

One immediate concern is the statistical significance of the difference in spread between the El Niño and La Niña composites. Although the patterns are distinct, could a single event or two result in the difference so as to render the disparity not statistically significant? For this reason, we present all five individual cases composing each composite for a close scrutiny of their generality, which will be presented promptly. Meanwhile, another way to assess the statistical significance of the reduction or increase in spread (natural variability) is

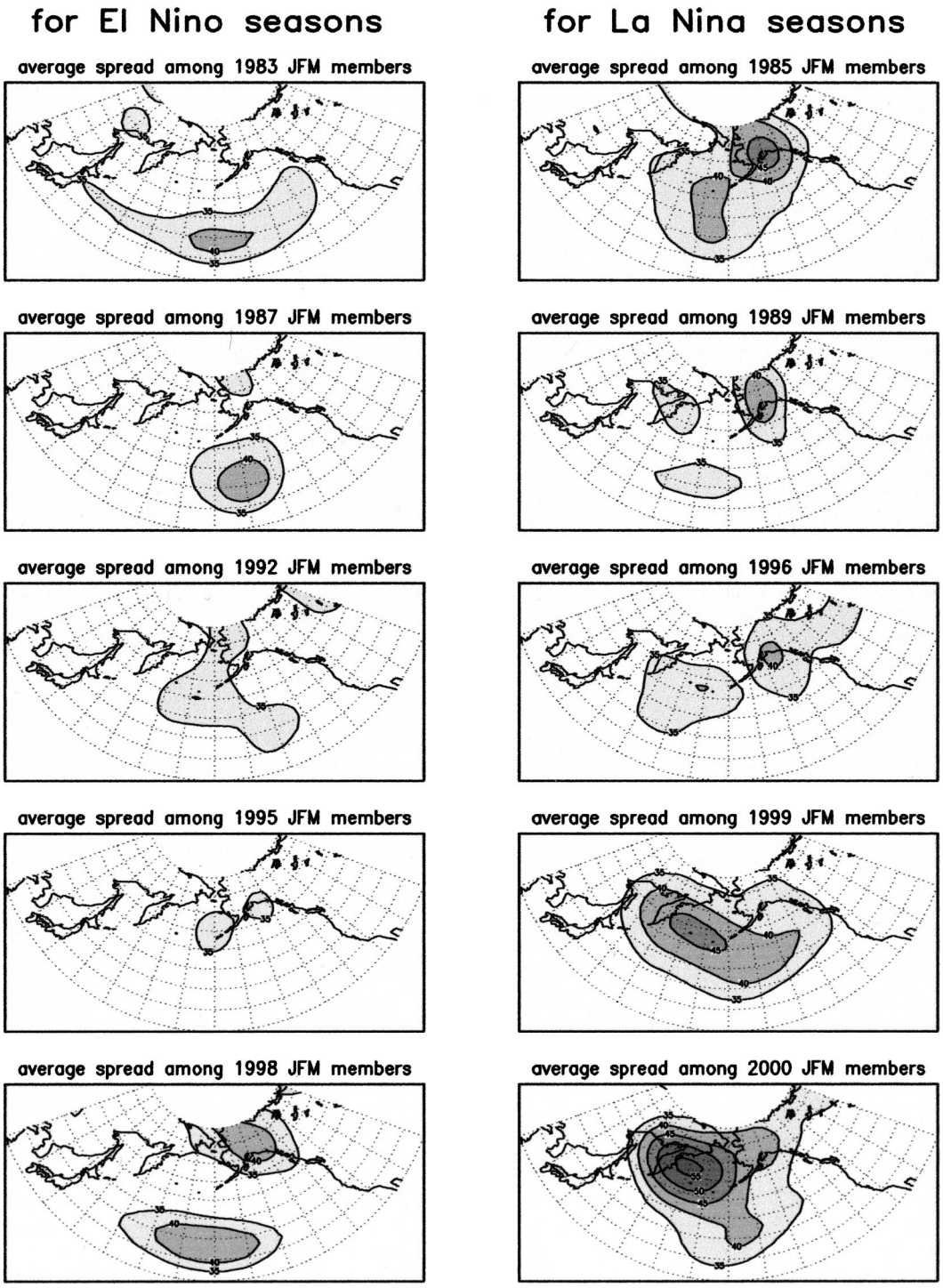

FIG. 8. Similar to Fig. 6 except for those of the T62 resolution model runs.

through an *F* distribution test. The results of such an exercise are also shown in Fig. 3.

The goal of the *F* test is to make certain that the natural variability during the warm (cool) phase of the ENSO cycle is significantly reduced (increased) from that during the neutral phase. In the middle-right panel of Fig. 3, the shaded region represent the variance ratio, var(El Niño)/var(neutral), that is less than unity. Similarly, a variance ratio greater than unity is represented by shaded area in the bottom-right panel for the variance ratio of var(La Niña)/var(neutral). The *F* values for certain specified significance levels can be found readily

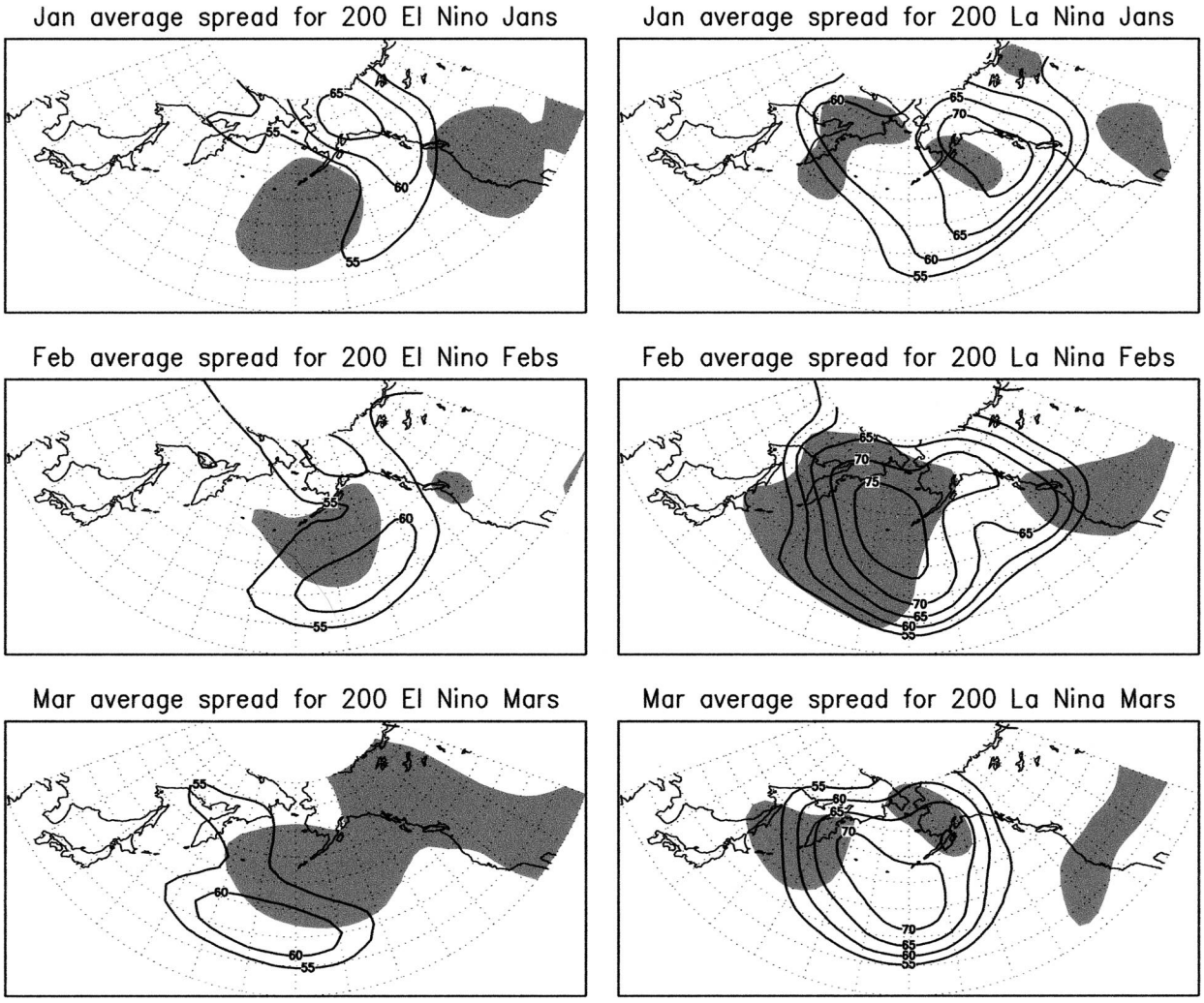

FIG. 9. Comparisons of spread magnitude, now on monthly time scales. Otherwise the datasets are the same as those used in Fig. 7. Again, the shaded areas represent regions where the spread variance ratio is statistically significant by *F* test at 0.05 level.

in most statistical manuals. For our case here, the number of degrees of freedom is 49 (5 events with 10 perturbations each minus 1) for El Niño and La Niña cases and 109 for neutral cases. In Fig. 3, the darker shades represent regions where the statistical significance of a decrease (or an increase) is at least at the 0.05 level. Contrasting the darker shades in Fig. 3, it is apparent that, over the North Pacific, the natural variability is significantly reduced during El Niño JFMs from neutral phases, while it is significantly increased during La Niña episodes. We note that the reduction during El Niño JFMs is more intense and extensive than the increase during La Niña JFMs. Nevertheless, an increase in natural variability during La Niña JFMs from neutral phases cannot be ignored. The increase is statistically significant at the 0.05 level for several large areas in the North Pacific.

As mentioned earlier, another way to look at a significant change in natural variability between El Niño and La Niña winters is to examine all individual cases instead of their composites, as shown in Fig. 4. Remarkably, most of the cases show large differences in their spread magnitude. The natural variability in El Niño cases is located mainly over the western North Pacific. In contrast, the larger variability in La Niña cases is located mainly over the central and the eastern North Pacific. Figure 4 offers a picture that is mostly consistent from one case to another.

The above results were from those hindcasts initialized from the preceding December. In addition to this set, there are numerous other hindcasts. Those initialized in November also yield a set of the JFM mean response and spread around its own ensemble mean. Furthermore, those initialized in October and September yield still another set each. Therefore, for the target JFM season, we have three more sets of spread similar to Figs. 3 and 4. The average of these four sets of composites is shown in Figs. 5 and 6. Very convincingly, Fig. 5 shows the

expected large differences in the magnitude of natural variability associated, respectively, with the El Niño and La Niña anomalous tropical forcing. We see that a significantly smaller magnitude of natural variability, on seasonal time scales, is associated with the El Niño events, while the La Niña events generated somewhat larger natural variability.

Similar to Fig. 4 in format, Fig. 6 contrasts the difference between individual JFM seasons for the average of four sets of hindcasts initialized from different months. Again, the difference in natural variability associated with El Niño versus La Niña anomalous forcing is rather distinct and convincing.

6. Hindcasts with T62 resolution as well as on monthly time scales

In 2001, the Seasonal Forecast Model was upgraded to T62 resolution from T42. In a similar fashion to Figs. 5 and 6, we evaluated the higher-resolution model data. The contrast of composites of natural variability is shown in Fig. 7. For individual ENSO events, the results are compared in Fig. 8. Note that four sets of ensemble runs, those initiated in September, October, November, and December, were used. Again, a distinct and large difference in natural variability on seasonal time scales between the El Niño and La Niña JFMs is observed. We note that, for the T62 resolution runs, the region of large natural variability shifts noticeably northward, especially in the western part of the North Pacific.

A large and significant change in natural variability on monthly time scales is also examined. Figure 9 contrasts the results for January, February, and March, respectively. Again, a large change in natural variability is robust and statistically significant.

7. Concluding remarks

As mentioned in the introduction, the assessments of modification in North Pacific natural variability associated with anomalous tropical forcing have not yielded a consistent result in the published literature. Since the omnipresent natural variability always degrades long-range predictions, this issue is of practical importance, beside being of an academic interest. The NCEP SFM's operational ensemble hindcasts offered another opportunity to reexamine this issue once again to help clarify the confusion. Four sets of 10-member ensemble hindcasts, those initialized in September, October, November, and December, with both T42 and T62 model resolutions, all yield a consistent picture. The results show convincingly that during El Niño (La Niña) winters the associated natural variability is distinctively smaller (larger) than those during neutral winters over the northeast Pacific. This result agrees well with the previous model studies and investigations using the NCEP–NCAR reanalysis (Chen and van den Dool 1995, 1997a,b, 1999; Lin and Derome 1996; Schubert et al. 2001). This reaffirmation implies that, during El Niño boreal winters, the predictability on both seasonal and monthly time scales is potentially higher than during La Niña winters over the North Pacific region where the ENSO signals are substantial and prominent.

Note that the results shown above were all obtained from the seasonal forecast model used here by NCEP, and, thus, may be unique to this particular model. As one of the reviewers pointed out, in so far as there is a noticeable model error in its climatological seasonal variance, as shown in Fig. 1, one can legitimately question whether this model's simulated changes in variance under ENSO influences are meaningful proxies for what occurs in nature.

Acknowledgments. The author would like to thank Drs. Marco Carrera, Jae Schemm, and Peitao Peng of CPC for reading and commenting on this article. He would also like to thank Dr. Martin Hoerling and two anonymous reviewers for their critical reviews. Their comments and suggestions have greatly improved the contents of this article.

REFERENCES

Alpert, J. C., M. Kanamitsu, P. M. Caplan, J. G. Sela, G. H. White, and E. Kalnay, 1988: Mountain induced gravity wave drag parameterization in the NMC medium-range model. Preprints, *Eighth Conf. on Numerical Weather Prediction,* Baltimore, MD, Amer. Meteor. Soc., 726–733.

Compo, G. P., P. D. Sardeshmukh, and C. Penland, 2001: Changes of subseasonal variability associated with El Niño. *J. Climate,* **14,** 3356–3374.

Chen, W. Y., and H. van den Dool, 1995: Low frequency variabilities for widely different basic flows. *Tellus,* **47A,** 526–540.

——, and ——, 1997a: Asymmetric impact of tropical SST anomalies on atmospheric internal variability over the North Pacific. *J. Atmos. Sci.,* **54,** 725–740.

——, and ——, 1997b: Atmospheric predictability of seasonal, annual, and decadal climate means and the role of the ENSO cycle: A model study. *J. Climate,* **10,** 1236–1254.

——, and ——, 1999: Significant change of extratropical natural variability and potential predictability associated with ENSO. *Tellus,* **51A,** 790–802.

Chow, M.-D., 1992: A solar radiation model for use in climate studies. *J. Atmos. Sci.,* **49,** 762–772.

Horel, J. D., and J. M. Wallace, 1981: Planetary scale atmospheric phenomena associated with the Southern Oscillation. *Mon. Wea. Rev.,* **109,** 813–829.

Hoskins, B. J., and D. J. Karoly, 1981: The steady linear response of a spherical atmosphere to thermal and orographic forcing. *J. Atmos. Sci.,* **38,** 1179–1196.

Kalnay, E., and Coauthors, 1996: The NCEP/NCAR 40-Year Reanalysis Project. *Bull. Amer. Meteor. Soc.,* **77,** 437–471.

Kanamitsu, M., and Coauthors, 2002: NCEP dynamical seasonal forecast system 2000. *Bull. Amer. Meteor. Soc.,* **83,** 1019–1037.

Kumar, A., A. G. Barnston, P. Peng, M. P. Hoerling, and L. Goddard, 2000: Changes in the spread of the variability of the seasonal mean atmospheric states associated with ENSO. *J. Climate,* **13,** 3139–3151.

Lin, H., and J. Derome, 1996: Changes in predictability associated with the PNA pattern. *Tellus,* **48A,** 553–571.

Moorthi, S., and M. J. Suarez, 1992: Relaxed Arakawa–Schubert: A parameterization of moist convection for general circulation models. *Mon. Wea. Rev.,* **120,** 978–1002.

Rasmusson, E. M., and J. M. Wallace, 1983: Meteorological aspects of the El Niño/Southern Oscillation. *Science,* **222,** 1195–1202.

Sardeshmukh, P. D., G. P. Compo, and C. Penland, 2000: Changes of probability associated with El Niño. *J. Climate,* **13,** 4268–4286.

Schubert, S. D., M. J. Suarez, Y. Chang, and G. Branstator, 2001: The impact of ENSO on extratropical low-frequency noise in seasonal forecasts. *J. Climate,* **14,** 2351–2365.

Slingo, J. M., 1987: The development and verification of a cloud prediction model for the ECMWF model. *Quart. J. Roy. Meteor. Soc.,* **113,** 899–927.

Wallace, J. M., and M. L. Blackmon, 1983: Observation of low-frequency atmospheric variability. *Large-Scale Dynamical Processes in the Atmosphere,* B. J. Hoskins and R. P. Pearce, Eds., Academic Press, 55–94.